



Decadal-scale soil redistribution along hillslopes in the Mojave Desert

O. Crouvi^{1,2}, V. O. Polyakov³, J. D. Pelletier², and C. Rasmussen⁴

¹Geological Survey of Israel, 30 Malkhe Israel St., Jerusalem 95501, Israel

²Department of Geosciences, University of Arizona, Tucson, AZ 85721, USA

³Southwest Watershed Research Center, USDA-ARS, 2000 E. Allen Rd., Tucson, AZ 85719, USA

⁴Department of Soil, Water, and Environmental Science, University of Arizona, Tucson, AZ 85721, USA

Correspondence to: O. Crouvi (crouvi@gsi.gov.il)

Received: 4 May 2014 – Published in Earth Surf. Dynam. Discuss.: 18 June 2014

Revised: 3 May 2015 – Accepted: 14 May 2015 – Published: 4 June 2015

Abstract. This study estimates the relative magnitude of decadal-scale soil redistribution (i.e., soil loss or gain) by slope wash using ^{137}Cs inventories measured in 46 soil profiles at four study sites in the Ft. Irwin area of the Mojave Desert of California, USA. The variability in ^{137}Cs inventories on a < 5 m scale suggests that even for the same topographic position, there is large variation in runoff generation and flow continuity. Smaller average ^{137}Cs inventories that are suggestive of higher relative erosion rates are associated with more gently sloping sites that have a lower percentage of surficial rock-fragment and vegetation coverage. Individual ^{137}Cs inventories from all four sites are positively correlated with the percentage of rock fragments in the upper soil profile. The increase in rock-fragment cover (i.e., soil armoring) with increasing slope gradient appears to negate any potential increase in transport effectiveness with increasing slope steepness. This armoring, together with the sandy-loam soil texture characteristic of steeper slopes, hinders runoff and slope-wash erosion. Our findings are supported by soil data that suggest that these patterns are persistent for longer timescales (i.e., centuries and millennia).

1 Introduction

Quantifying soil erosion rates and processes across different types of landscapes is essential to understanding how landscapes evolve under climatic, tectonic, and anthropogenic forcing. Although soil erosion is a natural process, it has intensified in the last century, mainly due to anthropogenic stressors (Montgomery, 2007). Thus, most efforts to quantify soil loss on decadal timescales have been concentrated on agricultural fields, whereas natural, uncultivated regions have been studied less intensively. In addition, soil erosion rates and processes are relatively well known for semiarid to humid regions throughout the world (e.g., Lal, 2001; Nearing et al., 2005; Verheijen et al., 2009) but have been less well studied in arid environments.

Surface (or slope) wash, induced by overland flow when the rainfall rate exceeds the infiltration capacity, contributes to soil erosion, especially in arid and semiarid regions where

vegetation is sparse and hillslope materials are relatively impermeable (e.g., Dietrich et al., 2003). Although transport laws for this process are not well established, sediment flux by flowing water is generally thought to be a positive function of both topographic gradient (slope) and contributing area, as the latter is a substitute for discharge (Dietrich et al., 2003; Dietrich and Perron, 2006). The positive relationship between slope and erosion rate is commonly used to model spatial and temporal changes in soil erosion rates (e.g., the slope-steepness factor in the Universal Soil Loss Equation (USLE) (Wischmeier and Smith, 1978) and in its extended form, the Revised Universal Soil Loss Equation (RUSLE) (Renard and Freimund, 1994)). Nevertheless, several field-based studies have suggested that the surficial cover on hillslopes might mask the otherwise positive correlation between slope and rates of erosion by slope wash. For example, a study from the hyperarid region of Israel found no clear rela-

relationship between slope gradient and runoff but found a negative correlation between slope and erosion rates (i.e., steeper slopes yield smaller erosion rates) (Yair and Klein, 1973). This inverse relationship was attributed to a difference in the fraction of the surface covered by rock fragments (herein represented as R_c). Similar findings were reported from semiarid sites in southeastern Arizona and the Sierra Nevada, California, showing that overland-flow velocities and erosion rates are only partly controlled by slope gradients and, more importantly, are related to differential R_c (Abrahams and Parsons, 1991; Nearing et al., 1999; Granger et al., 2001; Nearing et al., 2005), i.e., as R_c increases, the soil erosion rate decreases. Recently, a new compilation of erosion rate data (Cerdan et al., 2010) and a new soil erodibility map (Panagos et al., 2014) have shown the importance of R_c in decreasing soil erodibility and erosion rates in Europe, especially in Mediterranean countries. Larger R_c leads to lower erosion rates in potentially three ways (Poesen et al., 1994): (1) greater protection against raindrop impact and detachment of soil particles by slope wash, (2) a greater reduction in physical degradation of the underlying soil by hampering soil aggregate breakdown, surface sealing, and compaction, and (3) a reduction in flow velocity due to greater hydraulic roughness associated with the rock cover.

In contrast to the negative relationship between erosion rate and slope gradient, studies from an arid region in Israel suggest that a positive relationship exists between erosion and R_c and show that in areas with more pronounced rock coverage, soil erosion by slope wash increases (Yair and Enzel, 1987; Yair, 1990). Poesen et al. (1994) found that the net effect of R_c on soil erosion by water depends on the temporal and spatial scale considered, in that a negative relationship exists between sediment yield and R_c on the microplot and macroplot scales (4×10^{-6} – 10^0 m² and 10^1 – 10^4 m², respectively). However, on the mesoplot scale (10^{-2} – 10^2 m²), the relationship between R_c and sediment yield is more complex, and can be negative or positive depending on the structure of the topsoil and on the vertical position and size of the rock fragments (Poesen et al., 1994). The apparent complexity of the relationship between erosion rates and surface characteristics points to the need for additional data on soil erosion rates across multiple spatial scales in arid environments.

Most of the studies that have demonstrated the importance of R_c for soil erosion rates were conducted in semiarid to humid regions (i.e., those with a mean annual precipitation of >250 mm yr⁻¹). In arid regions (<250 mm yr⁻¹) our information on processes and rates of soil erosion by water on the hillslope scale is limited (but see Yair and Klein, 1973; Abrahams et al., 1984; Yair, 1990; Owen et al., 2011). In general, arid regions differ from semiarid regions in how both climatic and surficial properties affect erosion rates. Generally, the decrease in average annual rainfall across the semiarid to arid transition is accompanied by an even more pronounced decrease in vegetation coverage and an increase in R_c , whereas dust accretion rates are generally high in both regions (com-

pared to more humid climates) but vary locally (Birkeland, 1999; Laity, 2008). Due to these different characteristics, we cannot directly use the findings of prior studies on soil erosion rates and processes collected in semiarid to humid regions to make inferences about arid regions.

Inventories of the anthropogenic ¹³⁷Cs ($t_{1/2} = 30.2$ years) are widely used as tracers of soil movement in a wide range of environments in different regions of the world (e.g., Walling and He, 1999; Nearing et al., 2005; Kaste et al., 2006; O'Farrell et al., 2007). As the only source for ¹³⁷Cs is nuclear fission (fallout peak in 1963), this fallout nuclide is useful for calculating and tracing soil loss by flowing water over decadal (~ 50 -year) timescales. The technique relies on the assumption that ¹³⁷Cs is fixed to clay minerals on deposition, and any redistribution of ¹³⁷Cs relates to erosion and deposition processes in the landscape. Areas with relatively high amounts of ¹³⁷Cs are assumed to be areas of relative sediment accumulation, whereas areas with relatively low amounts of ¹³⁷Cs are assumed to have undergone erosion (or less aggradation, if the study area is aggradational). Several models have been developed for relating the vertical distribution of ¹³⁷Cs in soil profiles and the total amounts of ¹³⁷Cs across the landscape to erosion rates (e.g., Walling and He, 1999). To successfully relate ¹³⁷Cs profiles and inventories to absolute and relative erosion rates several assumptions should be met; the main challenge is finding a non-eroding and non-accumulating reference location to compare to eroding or aggrading sites (Parsons and Foster, 2011; Mabit et al., 2013).

Here we examine the distribution of ¹³⁷Cs along hillslopes in the Mojave Desert that have remained relatively free from anthropogenic disturbance. Our goals are to (1) quantify the relative abundance of ¹³⁷Cs in soils on scales of ~ 1 – 200 m on hillslopes with differing slope gradients and R_c , (2) examine whether topographic parameters, upslope contributing area, surficial rock coverage, and vegetation can explain the spatial distribution of ¹³⁷Cs inventories, and (3) use these relationships to gain insight into the erosion processes occurring in this landscape over the past 5 decades. We hypothesize that ¹³⁷Cs inventories in arid regions are partly controlled by R_c , similar to the case of semiarid regions. We chose six hillslopes in four sites in the Ft. Irwin area, California, that differ in vegetation and R_c and exhibit a wide range of topographic properties (slope and curvature); they thus serve as a suitable place to examine what variables control soil transport by slope wash. We then compared the ¹³⁷Cs inventories with soil catena data to gain insight into relative magnitudes of soil redistribution on longer timescales. Note that we assume that diffusion-like processes (e.g., bioturbation, creep) are barely active on short timescales, as the freeze–thaw cycling of wet soils that drives creep is relatively rare in this climate and the longevity of individual shrubs in the Mojave Desert is usually >70 – 100 years (Bowers et al., 1995); hence, vegetation turnover is not a dominant process on decadal scales. Thus, erosion by diffusion-like pro-

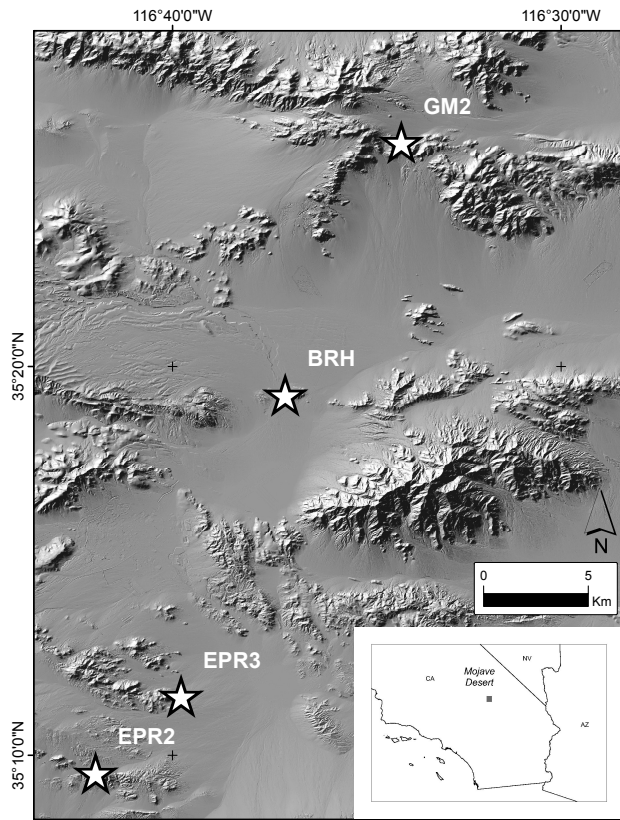


Figure 1. Location map of the four study sites (stars) in the southern part of Ft. Irwin, the Mojave Desert, southern CA. Topography from the lidar data is presented as shaded relief image.

cesses is likely not accounted for in ^{137}Cs inventories. As such, the decadal-scale ^{137}Cs inventories estimated here are mostly due to slope wash.

2 Materials and methods

2.1 Study area

The study area is located in the US Army National Training Center at Ft. Irwin, south-central California, in the western Mojave Desert (Fig. 1). The area is part of the Basin and Range Province, which is characterized by scattered mountain ranges rising sharply from wide alluvium-filled basins. Rocks within the study area are variable in lithology and age, but most outcrops are composed of Mesozoic plutonic rocks, which are the focus of this research. The climate of the region is arid, with hot and dry summers and warm and less dry winters. Precipitation is typically scarce and spotty, and varies from 110 to 150 mm yr⁻¹, mostly associated with winter Pacific frontal storms. The annual number of average days of high-intensity precipitation in the Mojave is 2.3 (high intensity is defined as precipitation > 90th percentile of all measurable daily precipitation at a station) (Griffiths et al.,

2006). The major vegetation types in the upland watersheds are the Mojave creosote bush scrub and the blackbrush scrub, which are dominated by creosote bush (*Larrea tridentata*), white bursage (*Ambrosia dumosa*), and blackbrush (*Coleogyne ramosissima*) (Fahnestock and Novak-Echenique, 2000).

The soils on upland watersheds are developed in residuum and colluvium from plutonic rocks and are well drained with a coarse sandy-loam to loam texture; they are classified as loamy-skeletal, mixed, superactive, calcareous, thermic Lithic Torriorthents and loamy-skeletal, mixed, mesic Lithic Haplargids (Fahnestock and Novak-Echenique, 2000). The soils exhibit high spatial variability in thickness that ranges from 20 to 150 cm (Crouvi et al., 2013). This variability is evident mostly in moderate to steep slopes ($\sim > 15^\circ$), in which extreme heterogeneity in soil thickness exists. In the upper and middle parts of these slopes, piles of boulders occur adjacent to areas covered with coarse to very coarse gravels (2–5 cm), which in turn cover soil by up to 1 m. The stages of carbonate morphology of the soils vary and range from stage I (undeveloped calcic soil) to stage IV (well-developed calcic soil with an indurated petrocalcic horizon) (Crouvi et al., 2013). The content of aeolian, external sediments in the upland soils is estimated to range from 50 to 100 % of the profiles, considering only the < 2 mm fraction of the soil; When considering the total soil thicknesses, including gravels (> 2 mm), aeolian materials make up 11 to 33 % of the total soil thickness (Crouvi et al., 2013).

3 Sampling

We chose four study sites in the study area (Figs. 1, 2). All sites are composed of plutonic rocks: two sites are composed of granite, one site of quartz monzonite (i.e., a quartz-poor granite), and one site of diorite (Table 1). The latter was selected in order to examine erosion rates in an intermediate igneous lithology, composed primarily of less weathering-resistant minerals (i.e., plagioclase feldspar). Slope gradient varies among the sites, and ranges from an average slope of 5° to a slope of 25°. Samples for ^{137}Cs analysis were collected during June 2011 along transects on NE- or NW-trending slopes for each site; additional SW-trending downslope transects were sampled for two of the sites. We sampled soil profiles for ^{137}Cs concentration along the transects in four topographic positions: summit, shoulder, backslope, and footslope (toeslope was not sampled) (Birkeland, 1999) (note that for one site, GM2, the summit is not the highest point in the area, but it is the highest point for the relevant transect). Sample intervals were 20 to 40 m between topographic positions (Figs. 2, 3). At each topographic position we dug and sampled two shallow soil profiles, separated by 1–5 m. Thus, a total of eight different soil profiles was sampled for each transect (except at one site, EPR3, in which one summit position was used for both transects). Soil was sampled at 3 cm intervals using a small shovel, reaching a maximum depth

Table 1. The study sites characteristics.

Site	GM2	EPR2	EPR3	BRH
Lithology and geologic period*	Quartz monzonite, Cretaceous	Diorite, Jurassic	Granite, Cretaceous	Granite, Jurassic–Cretaceous
Average slope (°), aspect, and length (m) of transects	25, NE, 130	16, NW, 130	7, NNE, 65 13, SSW, 85	5, NNW, 125 10, SW, 55
Elevation (m)	1260	910	750	780
Average rock cover (R_c) (> 0.5 m) (%) and SD	33 ± 13	27 ± 23	0	0
Average vegetation cover (%) and SD	52 ± 16	39 ± 9	20	10

* See Crouvi et al. (2013) for more details.

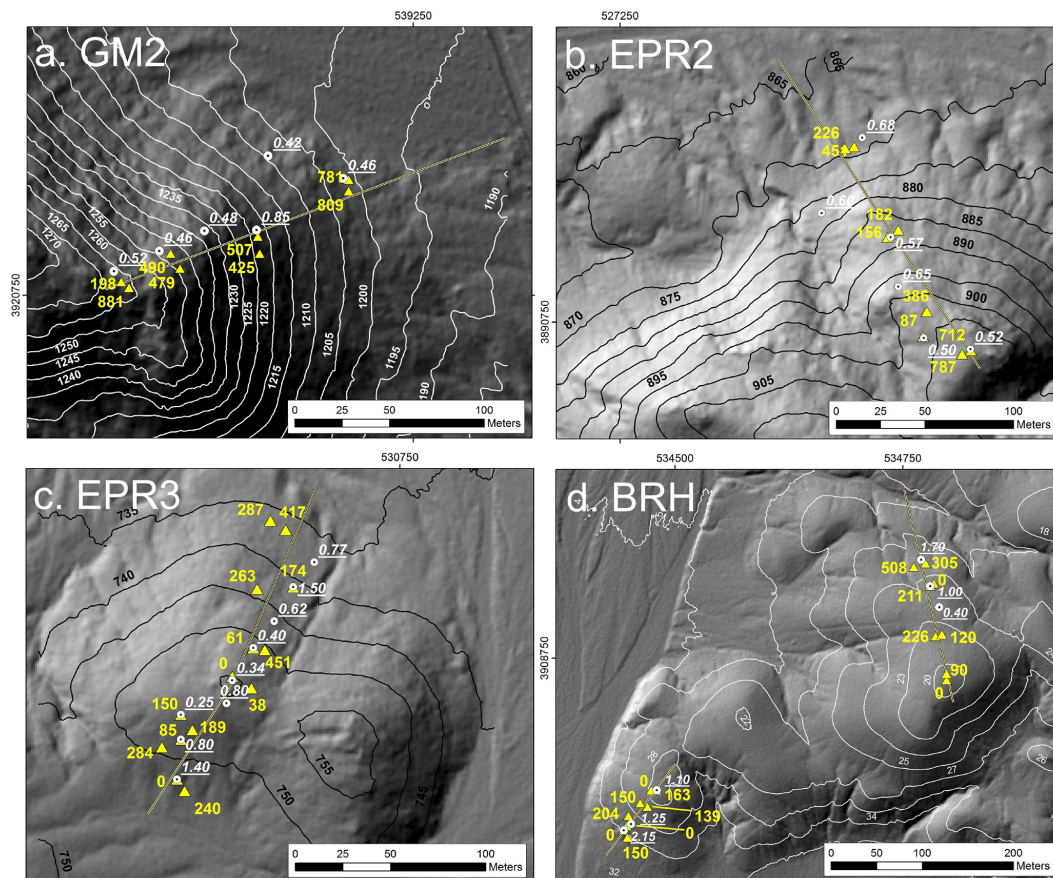


Figure 2. The spatial distribution of total ^{137}Cs inventories (Bq m^{-2}) per soil profile for each study site (yellow triangles and numbers): (a) GM2, (b) EPR2, (c) EPR3, (d) BRH north aspect, (e) BRH southwest aspect. Topographic transects are in yellow lines. Location and thickness (m) of studied soil pits (dug to bedrock) are represented by white circles and numbers. Topography from the lidar data is presented as contours and as shaded relief images.

of 9 cm. The total number of soil profiles and ^{137}Cs samples analyzed in this study is 46 and 138, respectively.

Soil properties, such as total thickness, thickness of A horizon, soluble-salt concentration and depth profile, and the

depth to the Bk horizon can help explain some of the variability in the relative magnitude of soil redistribution within each study site. Therefore, we dug 5–6 additional deep soil pits per transect (Fig. 2) using a hand shovel and a trencher. The

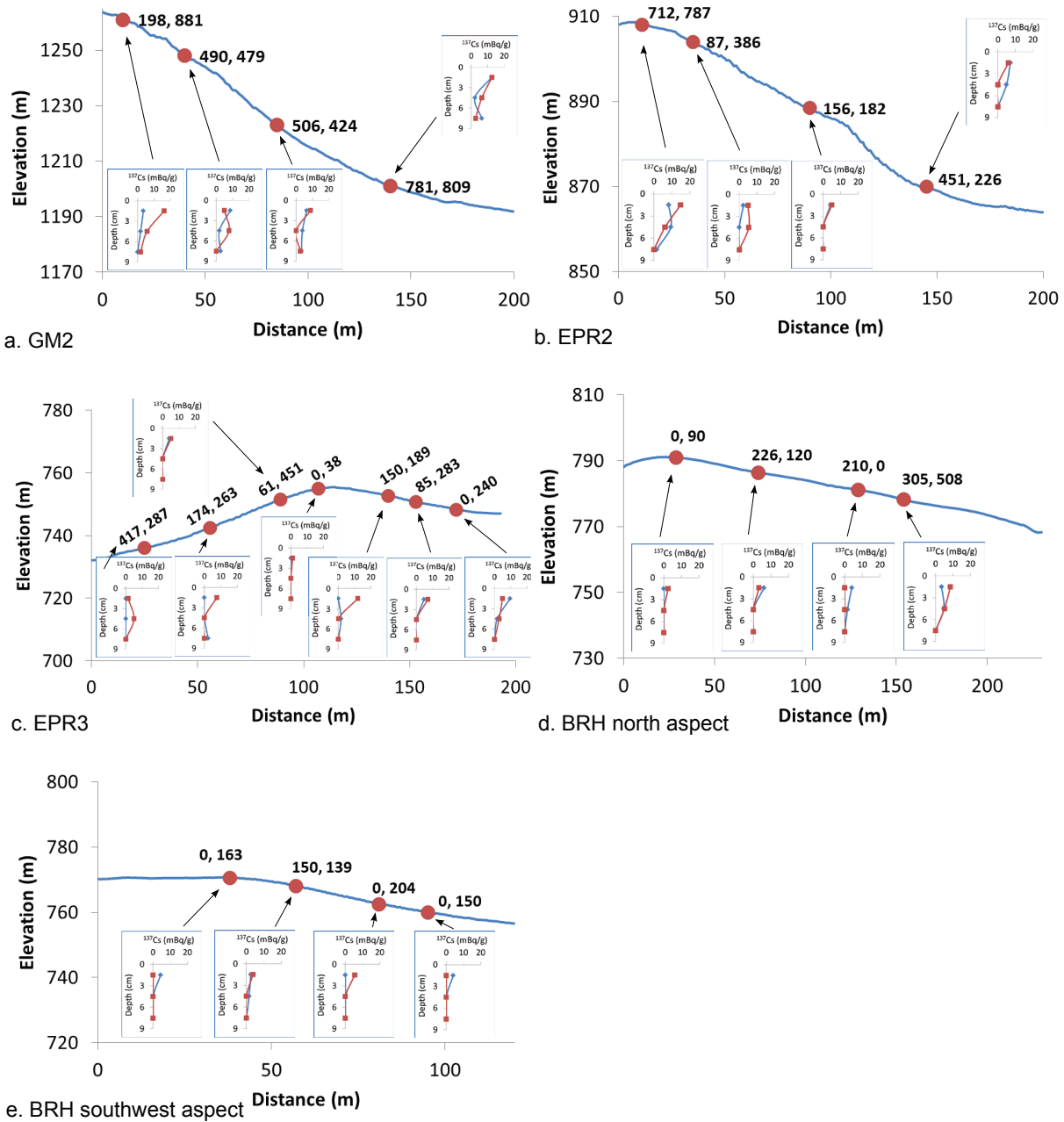


Figure 3. The distribution of total ^{137}Cs inventories (Bq m^{-2}) per soil pit along the hillslope for each study site: (a) GM2, (b) EPR2, (c) EPR3, (d) BRH, north aspect, (e) BRH southwest aspect. Insets show depth profiles in blue and red of ^{137}Cs activities (mBq g^{-1}) for the paired soil profiles sampled at each topographic position.

soil pits were dug down to the depth of unweathered bedrock (R horizon) defined as the “depth of refusal”, the point at which soil can no longer be excavated by hand, hydraulic core, or drill (Soil Survey Staff, 1999). The soils were described and sampled following standard methods (Soil Survey Staff, 1999). At each soil pit location at two of the sites, R_c was estimated by counting the number of rocks >0.5 m in diameter (both surface clasts and outcrop) in a 1 m interval along 50 m transect laid along the topographic contours

(Crouvi et al., 2013). R_c values for the other two less rocky sites were estimated visually. Vegetation coverage (including leaf area) was visually estimated for the area immediately surrounding each soil profile. In most transects we analyzed two profiles for particle size distribution (PSD), electrical conductivity (EC), and pH: one at the summit and one at the footslope. Samples were collected from genetic horizons which were brought back to the laboratory, air-dried, sieved with a 2 mm sieve, and split. Analysis of PSD was

carried out using a Beckman Coulter LS 13 320 laser diffraction particle size analyzer, following the procedure described in Crouvi et al. (2013). Organic matter was removed from the soil samples using NaOCl before the PSD analysis. Saturated soil pastes were extracted with the procedure outlined in Soil Survey Laboratory Staff (1999), and EC and pH were determined on saturation extracts immediately after extraction.

4 Analysis of ^{137}Cs in soil samples

Soil samples were dried and sieved through a 2 mm screen to break aggregates and homogenize the samples. The content of rock fragments (> 2 mm) by mass (herein R_m) in each soil profile was used as a proxy for the relative R_c upslope of the location of the soil profile (Nearing et al., 2005). The samples (< 2 mm) were weighed, placed into 120 mL tin cans in a uniform layer and sealed with an airtight lid. The depth of the samples in the cans was measured in order to calculate sample density. The analysis for ^{137}Cs was performed using a gamma ray spectrometry system consisting of two n-type high-purity closed-end coaxial germanium detectors (Canberra GC4019), with $> 30\%$ relative efficiency, coupled with an amplifier and a multichannel analyzer (DSA-2000A). The detectors were shielded with a 100 mm thick layer of lead. The system was calibrated using mixed radionuclide reference material IAEA-327 (Dekner, 1996), obtained from the International Atomic Energy Agency. The gamma emission spectrum was obtained over a 0–2 MeV range with a resolution of 0.24 keV (8192 channels). Measurement and spectrum analysis was conducted using the Genie-2000 Spectroscopy software (Canberra, 2009). The samples were counted for at least 80 000 s. The activity of ^{137}Cs (mBq g^{-1}) was calculated from the 661.6 keV photopeak. The analysis included a correction factor for self-attenuation due to the variation in sample volume and density (Quindos et al., 2006). To convert the ^{137}Cs activities (mBq g^{-1}) to ^{137}Cs inventories (Bq m^{-2}), we used a uniform bulk density of $1.25 \pm 0.16 \text{ g cm}^{-3}$. This value was calculated from the analyses of seven soil samples taken from the B horizon of the studied soils at the study sites (see Crouvi et al., 2013).

5 Estimating the topographical factors at sampling sites

We used a 1 m pixel^{-1} bare-earth digital elevation model (DEM) derived from airborne lidar to compute slope gradients, curvature values, and contributing areas. Prior to calculating these topographic properties using nearest-neighbor pixels, we smoothed the DEM using a moving average with a spatial scale of 5 m in order to partially remove small-scale variability, some of which includes real topographic variations (e.g., small outcrops) and some of which includes the small shrubs that cannot be perfectly differentiated from bare

Table 2. The ^{137}Cs inventories per soil profile for study sites.

	GM2	EPR2	EPR3	BRH
Mean, Bq m^{-2}	571.2	373.4	188.6	141.6
Minimum, Bq m^{-2}	198.0	86.7	0	0
Maximum, Bq m^{-2}	881.2	786.7	451.3	508.2
SD, Bq m^{-2}	232.1	261.6	144.2	136.8
SE, %	26	33	32	27
Number of samples	8	8	14	16

ground. This smoothing procedure greatly reduces the small-scale variability in the DEM without significantly affecting the shape of the landscape on the hillslope scale (Pelletier and Rasmussen, 2009; Pelletier et al., 2011). In the absence of such smoothing, the curvature data especially are entirely dominated by the local microtopography in a way that is unrealistic (i.e., curvature values oscillate wildly between positive and negative values independent of topographic position on the hillslope).

For each ^{137}Cs sampling location, we extracted the slope gradient and curvature value from the analysis. A positive curvature indicates that the surface is concave in that cell, whereas a negative curvature indicates that the surface is convex in that cell. A value of 0 indicates that the surface at the sampling point is locally planar. We calculated the Laplacian curvature using four nearest neighbors (i.e., the curvature in both directions of steepest descent and along-contour) (e.g., Roering et al., 1999). As curvature values calculated from a DEM are known to depend on the grid size (e.g., Heimsath et al., 1999), we examined a 5 m pixel^{-1} curvature map in addition to the 1 m pixel^{-1} values. According to Heimsath et al. (1999), curvature generally becomes scale independent at grid spacings or on spatial scales larger than 5 m, as most pit-and-mound topography occurs on spatial scales of less than 5 m. We also calculated a topographic proxy for shear stress by overland flow by multiplying the slope gradient by the square root of the contributing area (contributing area was calculated following the multiple-flow-direction algorithm of Freeman, 1991). This combination of slope and contributing area is a reasonable proxy for shear stress by overland flow since it predicts where channels begin, i.e., where incision by overland flow becomes more dominant over diffusive processes on hillslopes over geologic timescales (Montgomery and Dietrich, 1988).

6 Results

6.1 ^{137}Cs inventories

The ^{137}Cs mass activities and inventories in the soil samples varied greatly and for all depth increments ($n = 138$), ranging between 0 and 16.04 mBq g^{-1} and between 0 and 601.4 Bq m^{-2} , respectively (see Supplement).

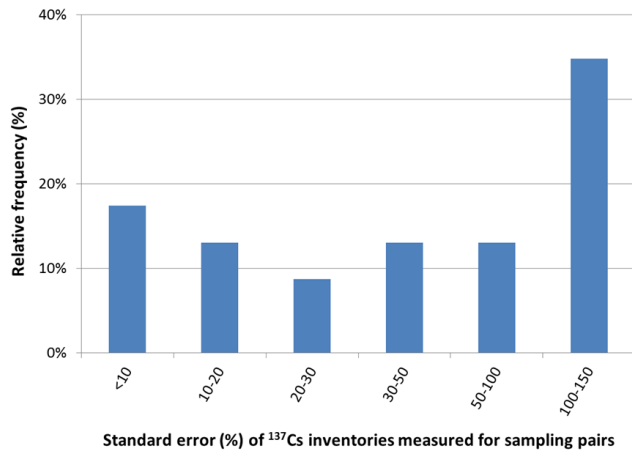


Figure 4. Relative frequency of the difference in standard error of a pair of ^{137}Cs inventories measured in the same topographic position.

In general, site GM2 exhibits the highest mean ^{137}Cs inventory of all study sites; site EPR2 (diorite) exhibits a lower mean value (Table 2). The two other sites, EPR3 and BRH, exhibit much lower mean values of ^{137}Cs inventory, including soil profiles in which no ^{137}Cs was detected. The ^{137}Cs depth profiles and total inventories on hillslopes vary within and between study sites (Figs. 2, 3). Differences in ^{137}Cs inventories between sampling pairs (located 1–5 m apart) vary significantly (Fig. 4): whereas half of the pairs shows standard errors less than 50 %, the other half exhibits much higher errors (50–150 %). At site GM2, all soil profile pairs show similar inventories at each topographic position. Most depth profiles exhibit detectable ^{137}Cs even at the shorter sampling interval (6–9 cm) (see insets in Fig. 3a). Some depth profiles are exponential, whereas others decrease from high surficial activities to steady activities at depth. At site EPR2 the two summit soil profiles show similar, high inventories; lower inventories are found downslope (Fig. 3b). For half of the soil profiles, ^{137}Cs activities were detected only at the uppermost sampling interval (0–3 cm), whereas for the rest, ^{137}Cs activities occur also at a depth of 3–6 cm, with zero to negligible activities at depth of 6–9 cm. Similar to site EPR2, site EPR3 exhibits variability in ^{137}Cs inventories in relation to topographic position for part of the profiles (Fig. 3c). Of the 14 profiles studied, 2 revealed no detectable ^{137}Cs activities at all, whereas for seven profiles, ^{137}Cs was detected only at a depth of 0–3 cm. Three profiles revealed detectable ^{137}Cs at a depth of 3–6 cm; two profiles exhibited no detectable ^{137}Cs at the surface and negligible activities at lower depths, which suggests the loss of the ^{137}Cs layer with subsequent deposition or other perturbation. At site BRH the ^{137}Cs inventories vary among topographic positions (Fig. 3d, e). Depth profiles are different than at the other sites, with overall low inventories found for this site. In 5 profiles out of the 16 studied, no ^{137}Cs is detected at all; for seven profiles

Table 3. Content of rock fragments by mass (R_m) (> 2 mm) in the soil profile (0–9 cm) for soils from the study sites.

	GM2	EPR2	EPR3	BRH
Mean, %	46.6	26.3	28.5	20.6
Minimum, %	40.3	9.8	16.3	0.9
Maximum, %	55.1	40.7	44.7	38.6
SD, %	5.2	10.2	8.6	10.3
SE, %	9.5	25.1	19.3	26.7
Number of samples	8	8	14	16

^{137}Cs is detected only at the surface. Only in four profiles is ^{137}Cs detected at a depth of 3–6 cm.

7 Effects of topographic factors and R_c on soil redistribution

Site GM2 exhibits the steepest topographic slopes at the sampling soil pits, ranging from 14 to 29°; slopes at site EPR2 range from 6 to 18°, from 5 to 15° at site EPR3, and from 2 to 12° at site BRH (Fig. 5a). Average negative curvature is the highest at site GM2 ($0.011 \pm 0.025 \text{ m}^{-1}$), followed by site EPR2 ($0.009 \pm 0.018 \text{ m}^{-1}$), site BRH ($0.007 \pm 0.006 \text{ m}^{-1}$), and site EPR3 ($0.005 \pm 0.010 \text{ m}^{-1}$) (Fig. 5b). Values of slope \times sqrt(contributing area) are mostly < 1.7 m, with a few exceptions at site GM2 (Fig. 5c). Within a given site, we found no significant relationship between ^{137}Cs inventories and topographic slope, between ^{137}Cs inventories and topographic curvature (both 1 and 5 m), or between ^{137}Cs inventories and slope \times sqrt (contributing area).

Since the number of samples at each study site is relatively low (8 to 16), we also examined the potential correlations using individual pits from all four study sites together, treating them as one sampling population. In doing so, we found a significant positive relationship between ^{137}Cs inventories and topographic slope (i.e., steeper slopes correlated to higher inventories) ($n = 46$; $r^2 = 0.14$; $p < 0.01$) (Fig. 5a). Moreover, when we perform this regression without the data of site EPR2, which is composed of a different (diorite) lithology, the relationship is even stronger ($n = 38$; $r^2 = 0.28$; $p < 0.001$). Similar positive significant relationships were observed between ^{137}Cs inventories and slope \times sqrt ($r^2 = 0.16$; $p < 0.01$ for all data; $r^2 = 0.29$; $p < 0.001$ for all data except for EPR2) (Fig. 5c). On the other hand, regressing the topographic curvature data (both 1 and 5 m) with or without the dioritic site against ^{137}Cs inventories reveals no significant correlation between these variables (Fig. 5b).

The average R_m at site GM2 is 46.6 %, i.e., much higher than at the other study sites (Table 3). Sites EPR2 and EPR3 show lower average R_m values, and BRH exhibits the lowest average R_m value (20.6 %). We found no significant relationship between ^{137}Cs inventories and R_m within each study site. However, when we examined all study sites together

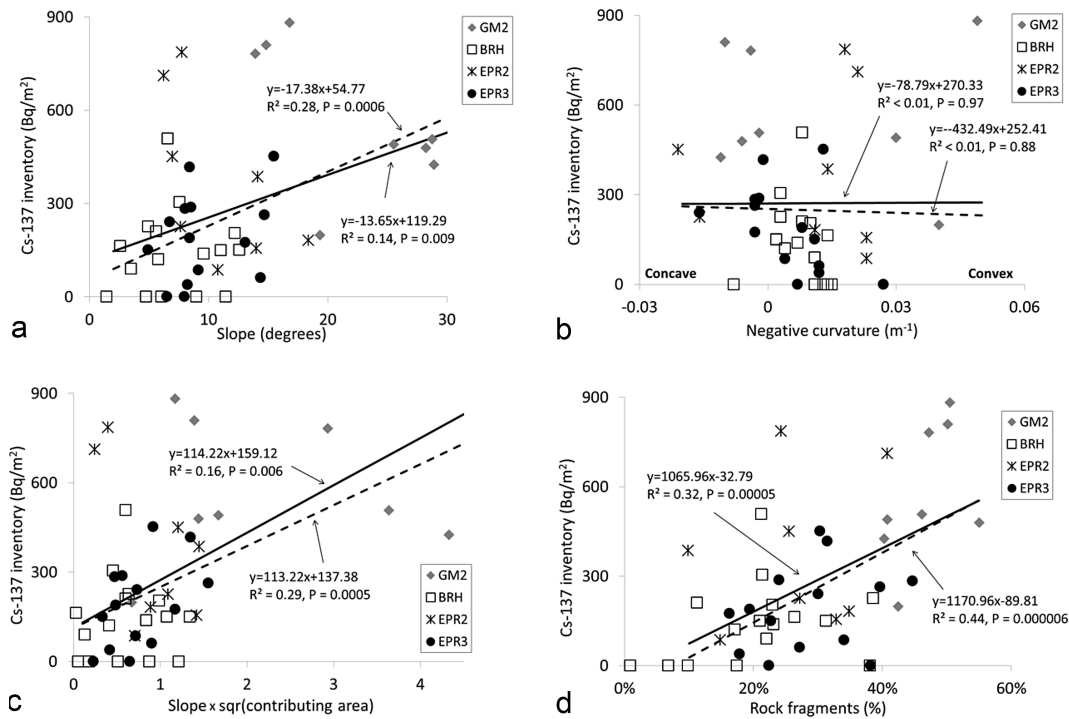


Figure 5. Relationships between total ^{137}Cs inventories (Bq m^{-2}) per soil pit and slope (a), curvature (b), slope \times sqrt(contributing area) (c), and rock fragments in soil R_m (d). Regressions of all data points appear as a black line; regressions of all data points except from site EPR2 appear as a dashed line. The curvature presented is calculated from 1 m pixel data; similar nonsignificant regressions were observed also for the 5 m pixel curvature data.

we found a significant positive linear relationship ($r^2 = 0.32$; $p < 0.0001$) (Fig. 5d). As for the slope data, the relationship is even stronger ($r^2 = 0.44$; $p < 0.00001$) when we do not account for the dioritic site. We should note that we did not observe any clear trend in vegetation coverage along hillslopes within sites.

8 Soil catena characteristics

Site GM2 is characterized by the highest average R_c and vegetation coverage of all studied sites (33 and 52 %, respectively) (Table 1). Most soils have A/Bk/Ck/R or A/Bk/BkC/R profiles; the backslope soil has an A/Bk/R profile. Soil thickness is relatively constant (40–50 cm), without a clear downslope trend along the 130 m catenary length (Fig. 6a) (the backslope profile is an exception, with 85 cm thick soil). The thickness of the A horizon (and thus the depth to the top of the Bk horizon) is relatively constant and ranges from 7 to 12 cm (except at the backslope profile). The soil texture of the A and Bk horizons changes from sandy loam at the summit to loamy sand at the footslope (Fig. 7). EC values for soil horizons at the summit are between 70 and $100 \mu\text{S cm}^{-1}$, whereas at the footslope they are higher and range from 200 to $400 \mu\text{S cm}^{-1}$ (Fig. 6a). In terms of carbonate morphology, the carbonate stage of the soils is mostly II, with slightly more developed soils (II–III) at the lower part of the slope.

Site EPR2 is characterized by slightly lower average R_c and vegetation coverage than site GM2 (27 and 39 %, respectively) (Table 1) but has a similar soil profiles. Soil thickness slightly increases downslope along the 130 m catenary length from ~ 50 cm to ~ 70 cm (Fig. 6b) (see also Crouvi et al., 2013). The A horizon is thin (~ 3 cm) and constant in thickness along the transect. The thickness and texture of the Bk horizon change downslope: at the summit the Bk horizon is 14 cm thick and of a loamy-sand to sandy-loam texture, whereas at the footslope it is 31 cm thick and of a sandy-loam texture (Figs. 6b, 8). Similar to the situation at site GM2, the footslope profile horizons accumulated more salts than the summit ($25\text{--}600$ vs. $2\text{--}300 \mu\text{S cm}^{-1}$, respectively) (Fig. 6b). The soils are relatively cobble- and gravel-poor (10–30 % in the A and B horizons) (Crouvi et al., 2013), are not well developed in terms of carbonate morphology (I–II), and have no clear trend in soil development downslope.

Site EPR3 is characterized by the absence of large (> 0.5 m) surficial rocks and a relatively low vegetation coverage (20 %). The soils at this site are more heterogeneous than the previously described sites. The summit soil has an A/Btk/R profile; the soils along the SSW transect have A/Bk/R or A/Bk/Ck/R profiles. Soil thickness gradually increases downslope along the 85 m catenary length from 34 cm at the summit to 77–150 cm in the lower parts of the slope (Fig. 6c) (see also Crouvi et al., 2013). Depth to top

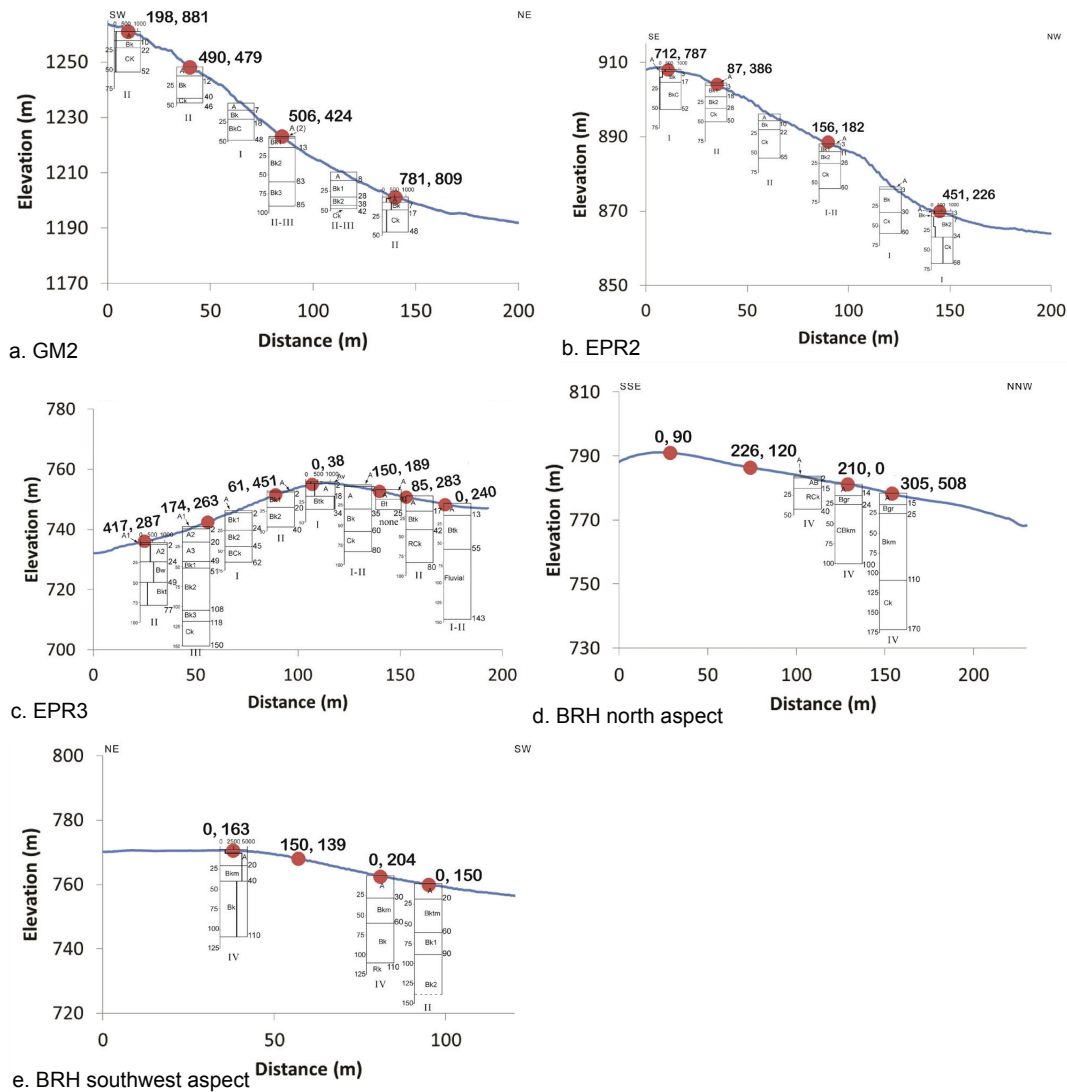


Figure 6. The distribution of total ^{137}Cs inventories (Bq m^{-2}) per soil pit along the hillslope for each study site: (a) GM2, (b) EPR2, (c) EPR3, (d) BRH north aspect, (e) BRH southwest aspect. The distribution of electrical conductivity values (EC) ($\mu\text{S cm}^{-1}$) with depth is presented for most of the summit and footslope profiles. Note scale difference for EC values at site BRH.

of the Bk horizon also increases from ~ 2 cm in the upper parts of the slopes to 40–50 cm at the bottom. The texture of the Btk horizon changes from sandy loam at the summit to clay loam at the base (Fig. 7). Cobble and gravel percentages range from 30 to 80% in the A and B horizons (see also Crouvi et al., 2013). EC values for soil horizons are higher than at previous sites ($50\text{--}1000 \mu\text{S cm}^{-1}$), whereas the summit profile exhibits higher EC values than the footslope (Fig. 6c). The soils show an increasing downslope trend in soil development, mostly with carbonate morphologic stage I in the upper parts of the slope and stages II and III in the lower parts. Most of the soils along the opposite and gently sloping NNE transect have a pronounced Bt horizon. Soil thickness changes from 25 to 80 cm without a clear trend downslope (Fig. 6c); fluvial deposits were observed at the

base of the footslope profile. The depth to the top of the Bk (or Btk) horizon (18–35 cm) and the carbonate morphologic stage (I to II) vary without a clear downslope trend. No PSD data are available for this transect.

Site BRH is characterized by gentle slopes and great variation in soil thickness from ~ 0.2 m on the flat summits to 1–1.7 m further downslope (Crouvi et al., 2013). The northward transect exhibit soils with a pronounced C horizon with A/AB/Ck, A/B/CBkm, and A/B/Bkm/Ck profiles (Fig. 6d). The soils along the southwest transect have an A/Bkm/Rk profile at the summit and an A/Bkm/Bk/Rk profile at the backslope. The footslope profile is similar to the backslope one, but fluvial sediments were found at the base of the pit (Fig. 6e). In both transects soil thickness increases downslope and the A horizon is relatively thick (15–30 cm) without

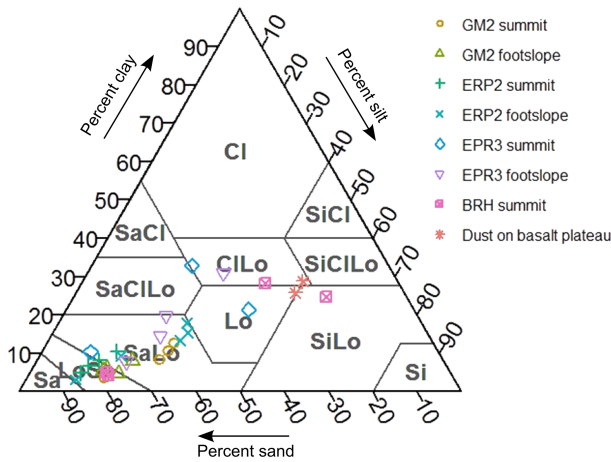


Figure 7. Particle size ternary plots and textural classes for the <2 mm fraction of A and B horizons of the studied soils. Abbreviations are as follows: Sa – sand; LoSa – loamy sand; SaLo – sandy loam; SaClLo – sandy clay loam; SaCl – sandy clay; Cl – clay; ClLo – clay loam; Lo – loam; SiCl – silty clay; SiClLo – silty clay loam; SiLo – silt loam; Si – silt.

signs of carbonate accumulation. In most soils the A horizons abruptly overlay the hard petrocalcic horizon (Bkm) that represents the greatest degree of carbonate morphology development found in this study (stages III–IV). At the summit, the soil texture of the A horizon is finer than at the other sites (clay–loam, loam to silt–loam) and resembles the texture of pure aeolian sediments that were sampled on a nearby basalt plateau (Crouvi et al., 2013) (Fig. 7). At this site EC values for the summit profile horizons are the highest measured in this study and range from 1000 to 4000 $\mu\text{S cm}^{-1}$.

9 Discussion

9.1 Processes that control the spatial patterns of ^{137}Cs inventories

The most striking observation is that ^{137}Cs inventories vary on all spatial scales: at 1–5 m (in between sampling pairs), at 20–200 m (on hillslopes), and at 5–30 km (between sites). We attribute this variability mainly to sediment transport by slope wash and not to other processes that can potentially transport sediments along hillslopes. Firstly, colluvial erosion and the slower downslope movement of soil due to creep and bioturbation are not likely to be captured using ^{137}Cs inventories that represent ~ 50 years of erosion. This is strengthened by the fact that we did not find a significant linear relationship between topographic curvature and ^{137}Cs inventories, as expected in any case in which soil redistribution is dominated by slope wash (Fig. 5b) (see also Nearing et al., 2005), whereas this relationship is significant when diffusive processes dominate (e.g., Heimsath et al., 2005; Roering, 2008; Pelletier and Rasmussen, 2009). Secondly, soil re-

distribution by wind is probably also not an important process as a) crusted topsoil is evident at all sites, b) upland soils serve as a sink for aeolian sediments (Crouvi et al., 2013), and c) the main sources of eolian sediments in the Mojave Desert are proximal and distal alluvial fans, washes, and playas (and not hillslopes) (e.g., Sweeney et al., 2013). Thirdly, we acknowledge the fact that, as stated above, there is a considerable eolian input to upland soils along the studied hillslopes (Crouvi et al., 2013). Except for unusual cases in which hillslopes are located very close to a localized aeolian source, the accumulation rate of dust transported in suspension can be and usually is assumed to be uniform unless the hillslope has a strong gradient in vegetation cover (Yan et al., 2011). The slopes we studied have had uniformly sparse vegetation cover (within a given site) since the time ^{137}Cs was deposited, and significant aeolian sources are ~ 1 –10 km from the hillslopes we studied, i.e., much larger than the 20–200 m scales separating our measurements within each hillslope. Fourthly, although there is a possibility that soil patches in rocky slopes contain more ^{137}Cs due to local wash of ^{137}Cs from adjacent outcrops, we think that this process is insignificant as the outcrops mostly drain into adjacent crevices. In addition, we sampled the ^{137}Cs from a pit that is 10×10 cm in size, and we avoided sampling near large clasts (> 10 cm). We assume that under these circumstances, the addition of wash off from small clasts (< 10 cm) is negligible in relation to a 10×10 cm size sampling area and cannot explain the overall trend in ^{137}Cs inventories along hillslopes, and the differences in average inventories between sites.

10 What controls the spatial patterns of ^{137}Cs inventories on different spatial scales?

The variability in erosion rates as inferred from ^{137}Cs inventories on a 1–5 m scale (Fig. 4) suggests that even for the same topographic position there is large variation in runoff generation and flow continuity at least for parts of the examined profiles. This is also emphasized by the great spatial variability in soil thickness we have previously reported (Crouvi et al., 2013) (see also below). Discontinuous runoff suggests that sediment along the hillslope is eroded locally, transported over a short distance and redeposited, as reported for other arid environments (e.g., Yair and Lavee, 1976; Lavee and Yair, 1990; Yair and Kossovsky, 2002). In this study we confirm that this variability also occurs when time periods of several decades are considered. The nature of the discontinuous runoff in arid regions is emphasized when we compare the standard errors found in this study of inventories sampled for pairs only 1–5 m apart (2–141 %) with those found in much wetter region (> 800 mm yr^{-1}) (8–42 %) (Kaste et al., 2006). The reason for this difference is attributed to both surface and rainfall characteristics (see also below) (e.g., Yair and Lavee, 1976; Lavee and Yair, 1990; Yair and Kossovsky, 2002).

The highly variable soil redistribution patterns are also evident on the 20–200 m scale as there is no clear trend in ^{137}Cs inventories downslope. However, our findings that individual ^{137}Cs inventories from all study sites are positively correlated with R_m implies that as the fraction of the surface covered with rock fragments (R_c) increases, soil erosion by water is less effective on average. The positive correlation between slope and ^{137}Cs inventories is the opposite of what we expected. We believe this correlation simply represents the fact that steeper slopes generally exhibit higher R_m (Pearson's $r = 0.57$ for all sites and 0.65 for all sites except EPR2; see also Tables 1, 4) (Abrahams et al., 1985; Hirmas et al., 2011). Thus, on steep slopes with abundant surficial rocks soil transport by water is less effective than on gentler slopes with limited abundance of rock fragments (Yair and Klein, 1973; Hirmas et al., 2011). Interestingly, the site with the diorite lithology does not exhibit extreme ^{137}Cs inventories; including this site in the analysis only slightly weakens the linear relationship between ^{137}Cs inventories and R_m (Fig. 5d). This suggests that the control of R_c on soil erosion is not limited only to granitic lithology but also relates to less weathering-resistant lithologies.

The positive correlation between slope and R_m has been attributed to past erosion: steeper slopes are believed to have undergone greater erosion in the past that removed fine material and increased rock cover (Poesen et al., 1998; Govers et al., 2006). Subsequently, an increase in rock cover leads to reduced soil erosion rates, eventually resulting in relatively uniform erosion rates across the hillslope (a state of slope–velocity equilibrium) (e.g., Govers et al., 2006). Thus, the control of R_c on ^{137}Cs inventories shown here, together with the apparent independence of direct control of slope gradient over ^{137}Cs inventories, are best explained in terms of hydraulic controls by the rocks and initial conditions of the sites and the associated slope–velocity equilibrium that develops on slopes (Nearing et al., 1999; Nearing et al., 2005). Clearly, the studied landscape did not yet reach a state of slope–velocity equilibrium as ^{137}Cs inventories (and hence soil erosion rates) vary within and between study sites. One possible reason is that these hillslopes have seen huge changes in the past 20 kyr (and longer) (for example, pinyon and juniper pine trees were abundant at these elevations (800 + m) at the Last Glacial Maximum).

Despite the fact that extreme small-scale variability in inventories was found that can significantly affect the inventories of individual pits, this tends to have less of an effect on the average of 8–16 pits (i.e., per site). Averaging the inventories across study sites reveals that the mean inventory is controlled mostly by rock and vegetation coverage (Tables 1, 2): sites with higher R_c and vegetation coverage exhibit higher ^{137}Cs inventories (GM2, EPR2), on average, compared to sites with mostly bare soil (EPR3, BRH). Note that as the mean coverage percentage of rock and vegetation are positively correlated, we relate the difference in mean ^{137}Cs inventories between sites to the combined ef-

fect of rock and vegetation cover as we cannot differentiate between the two here. However, since we did not observe any downslope change in vegetation cover within sites, vegetation alone cannot explain the variability in soil erosion rates within sites; thus, our interpretation of the significant relationship between rock fragment content in individual soil profiles vs. ^{137}Cs inventories is that these inventories can be explained, at least partly, by rock coverage percentage.

Our interpretation that higher R_c and vegetation coverage decreases the magnitude of soil redistribution by slope wash is in agreement with previous studies that were performed in more humid climates (Poesen et al., 1994; Riebe et al., 2000; Cerda, 2001; Granger et al., 2001; Nearing et al., 2005). However, studies from a different arid region (Israel) (Yair and Enzel, 1987; Yair, 1990) found a positive relationship between R_c and soil erosion by water, the opposite of our findings. The reason for this discrepancy is most likely related to a difference in lithology and subsequently in surficial rock size and position in the soil (see Fig. 7 in Poesen et al., 1994). On the hillslopes studied here 1) most of the plutonic rocks are not well embedded in the soil, creating large spaces in between boulders and crevices, which favors a high infiltration rate, and 2) the topsoil texture is mostly sandy loam (with 60–75% sand; Fig. 7) which originates from the in situ weathering of the rocks and from aeolian input from sand-rich washes, promoting infiltration and depressing runoff as compared to surfaces with a silt-rich crust (e.g., Kidron et al., 2012). On the other hand, in the Negev Desert the carbonate bedrock is usually well embedded in the soil, and the soil is composed mostly of pure silt-sized dust particles with a loamy texture.

11 Implications for soil development on arid hillslopes

Our results suggest that the spatial variability ^{137}Cs inventories that represent decadal-scale soil transport by slope wash are also manifested in the soil catena data. In general, low ^{137}Cs inventories suggest high soil erosion rates, relatively high runoff, and low infiltration, resulting in less water infiltrating the soil compared with soils located in areas with high ^{137}Cs inventories (i.e., low erosion rates). Limited water infiltration will lead to high concentrations of soluble salts located at shallow depths; higher erosion rates will also lead to thinner soils, thinner A and C horizons, and shallower depths to the Bk horizon, all else being equal. Moreover, we expect that variable soil erosion rates along a hillslope will lead to great variation in the abovementioned soil properties. At site GM2, the relatively uniform soil thickness and depth to Bk horizon, the presence of weathered C horizon, and the limited amount of soluble salts in the profiles suggest that relatively large (compared to the other studied sites) and uniform amounts of water infiltrate the soil. These are in agreement with our findings of high and relatively constant ^{137}Cs

inventories. At the dioritic site (EPR2), soil characteristics do not change dramatically downslope and are in agreement with the relatively uniform ^{137}Cs inventories, which are intermediate in magnitude among the sites. Soils profiles in EPR3 are diverse in terms of profile horization, depth to Bk horizon, and thickness. Most profiles lack the C and Bk horizons and exhibit more clay-rich B horizons (Bt) with a relatively high soluble-salt content that directly overlays the unweathered bedrock (R horizon), suggesting limited infiltration and high erosion rates (low ^{137}Cs inventories). On the other hand, few soils exhibit a clear C horizon underlying the Bk horizon. Overall, the soil data suggest high and varied erosion rates along the hillslopes, with different amounts of water infiltrating the soils, in agreement with the ^{137}Cs results. At site BRH, most profiles present buried soil with well-developed calcic and petrocalcic horizons (Bkm horizon; carbonate stages II–IV) (see also Crouvi et al., 2013). These profiles are abruptly overlain by a soil profile composed mostly of a 15–30 cm thick A horizon. The lack of recent accumulation of pedogenic carbonate at the upper 30 cm of the soils (as opposed to what was found in the other studied sites), together with the high content of soluble salts, suggests that a limited amount of water infiltrated the soil. Thus, soil data suggest high runoff coefficients and erosion rates, as found using the ^{137}Cs inventories. In addition, this site exhibits a loamy texture for the A and A/B horizons, which promotes runoff and erosion. Thus, the good agreement between the observed patterns of ^{137}Cs inventories and the soil data suggests that these decadal-scale patterns probably represent century to millennial scales.

12 Conclusions

The results of this study show that in the Ft. Irwin area of the Mojave Desert, the relative magnitudes of soil redistribution by slope wash along hillslopes are mainly controlled by surficial rock coverage, similar to findings from semiarid regions (e.g., the Sonoran Desert). Steep slopes are characterized by higher rock and vegetation coverage and exhibit lower soil loss rates compared to gentle slopes that are characterized by mostly bare soil. As the slopes get rockier as they get steeper, the magnitude of soil loss increases, despite the tendency towards greater transport effectiveness on steeper slopes. The abundance on steep slopes of large plutonic rock fragments that are not well embedded in the soil creates large spaces in between boulders and cracks that favors a high infiltration rate. This, together with the sandy-loam topsoil texture, hinders runoff and erosion.

The Supplement related to this article is available online at doi:10.5194/esurf-3-251-2015-supplement.

Acknowledgements. We thank Ruth Sparks and Dave Housman from ITAM, Ft. Irwin, for helping with the logistics and permits for the field trips. We thank Mercer Meding, Justine Peal Mayo, Natalie Lucas, Chris Clingensmith, and Stephanie Castro for helping with the laboratory analyses. We wish to thank Aaron Yair from the Hebrew University for reviewing an early draft of this manuscript. We also thank associate editor Gerard Govers and two anonymous reviewers for their comprehensive comments that helped to improve the manuscript. This study was funded by the Terrestrial Sciences Program of the Army Research Office under grant number 55104-EV and was supported by NSF EAR/IF #0929850.

Edited by: G. Govers

References

- Abrahams, A. D. and Parsons, A. J.: Relation between sediment yield and gradient on debris-covered hillslopes, Walnut Gulch, Arizona, *Geol. Soc. Am. Bull.*, 103, 1109–1113, 1991.
- Abrahams, A. D., Parsons, A. J., Cooke, R. U., and Reeves, R. W.: Stone movement on hillslopes in the Mojave Desert, California: a 16 year record, *Earth Surf. Proc. Land.*, 9, 365–370, 1984.
- Abrahams, A. D., Parsons, A. J., and Hirsh, P. J.: Hillslope gradient-particle size relations: evidence for the formation of debris slopes by hydraulic processes in the Mojave Desert, *J. Geol.*, 93, 347–357, 1985.
- Birkeland, P. W.: *Soils and Geomorphology*, Oxford University Press, New York, 430 pp., 1999.
- Bowers, J. E., Webb, R. H., and Rondeau, R. J.: Longevity, recruitment and mortality of desert plants in Grand Canyon, Arizona, USA, *J. Veg. Sci.*, 6, 551–564, doi:10.2307/3236354, 1995.
- Cerda, A.: Effects of rock fragment cover on soil infiltration, interrill runoff and erosion, *Eur. J. Soil Sci.*, 52, 59–68, 2001.
- Cerdan, O., Govers, G., Le Bissonnais, Y., Van Oost, K., Poesen, J., Saby, N., Gobin, A., Vacca, A., Quinton, J., Auerswald, K., Klik, A., Kwaad, F. J. P. M., Raclot, D., Ionita, I., Rejman, J., Rousseva, S., Muxart, T., Roxo, M. J., and Dostal, T.: Rates and spatial variations of soil erosion in Europe: A study based on erosion plot data, *Geomorphology*, 122, 167–177, doi:10.1016/j.geomorph.2010.06.011, 2010.
- Crouvi, O., Pelletier, J. D., and Rasmussen, C.: Predicting the thickness and aeolian fraction of soils in upland watersheds of the Mojave Desert, *Geoderma*, 195–196C, 94–110, 2013.
- Dekner, R.: *Intercomparison Run IAEA-326 and IAEA-327 Radionuclides in Soil*, Analytical Quality Control Services, Vienna, Austria, 1996.
- Dietrich, W. E. and Perron, T.: The search for a topographic signature of life, *Nature*, 439, 411–418, 2006.
- Dietrich, W. E., Bellugi, D. G., Sklar, L. S., Stock, J. D., Heimsath, A. M., and Roering, J. J.: Geomorphic transport laws for predicting landscape form and dynamics, *Pred. Geomorphol.*, 103–132, 2003.
- Fahnestock, P. B. and Novak-Echenique, P.: *Soil Survey of National Training Center, Fort Irwin, California*, USDA, NRCS, 730, 2000.
- Freeman, T. G.: Calculating catchment area with divergent flow based on a regular grid, *Comput. Geosci.*, 17, 413–422, 1991.

- Govers, G., Van Oost, K., and Poesen, J.: Responses of a semi-arid landscape to human disturbance: A simulation study of the interaction between rock fragment cover, soil erosion and land use change, *Geoderma*, 133, 19–31, 2006.
- Granger, D. E., Riebe, C. S., Kirchner, J. W., and Finkel, R.: Modulation of erosion on steep granitic slopes by boulder armoring, as revealed by cosmogenic ^{26}Al and ^{10}Be , *Earth Planet. Sc. Lett.*, 186, 269–281, 2001.
- Griffiths, P. G., Hereford, R., and Webb, R. H.: Sediment yield and runoff frequency of small drainage basins in the Mojave Desert, USA, *Geomorphology*, 74, 232–244, 2006.
- Heimsath, A., Dietrich, W., Nishiizumi, K., and Finkel, R. C.: Cosmogenic nuclides, topography, and the spatial variation of soil depth, *Geomorphology*, 27, 151–172, 1999.
- Heimsath, A., Furbish, D. J., and Dietrich, W.: The illusion of diffusion: field evidence for depth-dependent sediment transport, *Geology*, 33, 949–952, 2005.
- Hirmas, D. R., Graham, R. C., and Kendrick, K. J.: Soil-geomorphic significance of land surface characteristics in an arid mountain range, Mojave Desert, USA, *Catena*, 87, 408–420, 2011.
- Kaste, J. M., Heimsath, A., and Hohmann, M.: Quantifying sediment transport across an undisturbed prairie landscape using cesium-137 and high resolution topography, *Geomorphology*, 76, 430–440, 2006.
- Kidron, G. J., Monger, C. H., Vonshak, A., and Conrod, W.: Contrasting effects of microbiotic crusts on runoff in desert surfaces, *Geomorphology*, 139–140, 484–494, 2012.
- Laity, J. J.: *Deserts and Desert Environments*, Wiley-Blackwell, 2008.
- Lal, R.: Soil degradation by erosion, *Land Degrad. Dev.*, 12, 519–539, 2001.
- Lavee, H. and Yair, A.: Spatial variability of overland flow in a small arid basin, *Erosion, Transport and Deposition Processes*, Jerusalem, Israel, 105–120, 1990.
- Mabit, L., Meusburger, K., Fulajtar, E., and Alewell, C.: The usefulness of ^{137}Cs as a tracer for soil erosion assessment: a critical reply to Parsons and Foster (2011), *Earth-Sci. Rev.*, 127, 300–307, 2013.
- Montgomery, D. R.: Soil erosion and agricultural sustainability, *P. Natl. Acad. Sci.*, 104, 13268–13272, 2007.
- Montgomery, D. R. and Dietrich, W. E.: Where do channels begin?, *Nature*, 336, 232–234, 1988.
- Nearing, M. A., Simanton, J. R., Norton, L. D., Bulygin, S. J., and Stone, J.: Soil erosion by surface water flow on a stony, semiarid hillslope, *Earth Surf. Proc. Land.*, 24, 677–686, 1999.
- Nearing, M. A., Kimoto, A., Nichols, M. H., and Ritchie, J. C.: Spatial patterns of soil erosion and deposition in two small, semiarid watersheds, *J. Geophys. Res.*, 110, F04020, doi:10.1029/2005JF000290, 2005.
- O’Farrell, C. R., Heimsath, A., and Kaste, J. M.: Quantifying hillslope erosion rates and processes for a coastal California landscape over varying timescales, *Earth Surf. Proc. Land.*, 32, 544–560, 2007.
- Owen, J., Amundson, R., Dietrich, W., Nishiizumi, K., Sutter, B., and Chong, G.: The sensitivity of hillslope bedrock erosion to precipitation, *Earth Surf. Proc. Land.*, 36, 117–135, 2011.
- Panagos, P., Meusburger, K., Ballabio, C., Borrelli, P., and Alewell, C.: Soil erodibility in Europe: A high-resolution dataset based on LUCAS, *Sci. Tot. Environ.*, 479–480, 189–200, doi:10.1016/j.scitotenv.2014.02.010, 2014.
- Parsons, A. J. and Foster, R. C.: What can we learn about soil erosion from the use of ^{137}Cs ?, *Earth-Sci. Rev.*, 108, 101–113, 2011.
- Pelletier, J. D. and Rasmussen, C.: Geomorphically based predictive mapping of soil thickness in upland watersheds, *Water Resour. Res.*, 45, W09417, doi:10.1029/2008WR007319, 2009.
- Pelletier, J. D., McGuire, L. A., Ash, J. L., Engelder, T. M., Hill, L. E., Leroy, K. W., Orem, C. A., Rosenthal, S. W., Trees, M. A., Rasmussen, C., and Chorover, J.: Calibration and testing of upland hillslope evolution models in a dated landscape: Banco Bonito, New Mexico, USA, *J. Geophys. Res.*, 116, F04004, doi:10.1029/2011JF001976, 2011.
- Poesen, J. W., Torri, D., and Bunte, K.: Effects of rock fragments on soil erosion by water at different spatial scales: a review, *Catena*, 23, 141–166, 1994.
- Poesen, J. W., van Wesemael, B., Bunte, K., and Benet, A. S.: Variation of rock fragment cover and size along semiarid hillslopes: a case-study from southeast Spain, *Geomorphology*, 23, 323–335, doi:10.1016/S0169-555X(98)00013-0, 1998.
- Quindos, L. S., Sainz, C., Fuente, I., Nicolas, J., Quindos, L., and Arteche, J.: Correction by self-attenuation in gamma-ray spectrometry for environmental samples, *J. Radioanal. Nucl. Ch.*, 270, 339–343, 2006.
- Renard, K. G. and Freimund, J. R.: Using monthly precipitation data to estimate the R-factor in the revised USLE, *J. Hydrol.*, 157, 287–306, 1994.
- Riebe, C. S., Kirchner, J. W., Granger, D. E., and Finkel, R. C.: Erosional equilibrium and disequilibrium in the Sierra Nevada, inferred from cosmogenic (super 26) Al and (super 10) Be in alluvial sediment, *Geology*, 28, 803–806, 2000.
- Roering, J. J.: How well can hillslope evolution models “explain” topography? Simulating soil transport and production with high-resolution topographic data, *Geological Society of America Bulletin*, 120, 1248–1262, 2008.
- Roering, J. J., Kirchner, J. W., and Dietrich, W.: Evidence for non-linear, diffusive sediment transport on hillslopes and implications for landscape morphology, *Water Resources Research*, 35, 853–870, 1999.
- Soil Survey Staff: *Soil Taxonomy: a Basic System of Soil Classification for Making and Interpreting Soil Surveys*, USDA Natural Resource Conservation Service Agriculture, US Government Printing Office, Washington DC, 1999.
- Sweeney, M. R., McDonald, E., and Markley, C. E.: Alluvial sediment or playas: What is the dominant source of sand and silt in desert soil vesicular A horizons, southwest USA, *J. Geophys. Res.*, 118, 257–275, doi:10.1002/jgrf.20030, 2013.
- Verheijen, F. G. A., Jones, R. J. A., Rickson, R. J., and Smith, C. J.: Tolerable vs. actual soil erosion rates in Europe, *Earth-Sci. Rev.*, 94, 23–38, 2009.
- Walling, D. E. and He, Q.: Improved models for estimating soil erosion rates from cesium-137 measurements, *J. Environ. Qual.*, 28, 611–622, 1999.
- Wischmeier, W. H. and Smith, D. D.: *Predicting Rainfall Erosion Losses: a Guide to Conservation Planning*, USDA/Science and Education Administration, US Gov. Printing Office, Washington, DC, 58, 1978.

- Yair, A.: The role of topography and surface cover upon soil formation along hillslopes in arid climates, *Geomorphology*, 3, 287–299, 1990.
- Yair, A. and Klein, M.: The influence of surface properties on flow and erosion processes on debris covered slopes in an arid area, *Catena*, 1, 1–14, 1973.
- Yair, A. and Lavee, H.: Runoff generative process and runoff yield from arid talus mantled slopes, *Earth Surf. Proc.*, 1, 235–247, 1976.
- Yair, A. and Enzel, Y.: The relationship between annual rainfall and sediment yield in arid and semi-arid areas; the case of the northern Negev, *Catena*, 10, 121–135, 1987.
- Yair, A. and Kossovsky, A.: Climate and surface properties; hydrological response of small arid and semi-arid watersheds, *Geomorphology*, 42, 43–57, 2002.
- Yan, Y., Xu, X., Xin, X., Yang, G., Wang, X., Yan, R., and Chen, B.: Effect of vegetation coverage on aeolian dust accumulation in a semiarid steppe of northern China, *Catena*, 87, 351–356, doi:10.1016/j.catena.2011.07.002, 2011.